The Astrophysical Journal Letters, 756:L34 (5pp), 2012 September 10 doi:10.1088/2041-8205/756/2/L34
© 2012. The American Astronomical Society. All rights reserved. Printed in the U.S.A.

ON THE WEAK-WIND PROBLEM IN MASSIVE STARS: X-RAY SPECTRA REVEAL A MASSIVE HOT WIND IN μ COLUMBAE

David P. Huenemoerder[1], Lidia M. Oskinova[2], Richard Ignace[3], Wayne L. Waldron[4], Helge Todt[2], Kenji Hamaguchi[5,6], and Shunji Kitamoto[7]
[1] Massachusetts Institute of Technology, Kavli Institute for Astrophysics and Space Research, 70 Vassar Street, Cambridge, MA 02139, USA
[2] Institute for Physics and Astronomy, University of Potsdam, D-14476 Potsdam, Germany
[3] Department of Physics and Astronomy, East Tennessee State University, Johnson City, TN 37614, USA
[4] Eureka Scientific Inc., 2452 Dellmer Street, Suite 100, Oakland, CA 94602, USA
[5] CRESST and X-ray Astrophysics Laboratory, NASA/GSFC, Greenbelt, MD 20771, USA
[6] Department of Physics, University of Maryland, Baltimore County, 1000 Hilltop Circle, Baltimore, MD 21250, USA
[7] Department of Physics, Rikkyo University, Tokyo 171-8501, Japan
Received 2012 June 16; accepted 2012 August 3; published 2012 August 22

ABSTRACT

μ Columbae is a prototypical weak-wind O star for which we have obtained a high-resolution X-ray spectrum with the *Chandra* LETG/ACIS instrument and a low-resolution spectrum with *Suzaku*. This allows us, for the first time, to investigate the role of X-rays on the wind structure in a bona fide weak-wind system and to determine whether there actually is a massive hot wind. The X-ray emission measure indicates that the outflow is an order of magnitude greater than that derived from UV lines and is commensurate with the nominal wind–luminosity relationship for O stars. Therefore, the "weak-wind problem"—identified from cool wind UV/optical spectra—is largely resolved by accounting for the hot wind seen in X-rays. From X-ray line profiles, Doppler shifts, and relative strengths, we find that this weak-wind star is typical of other late O dwarfs. The X-ray spectra do not suggest a magnetically confined plasma—the spectrum is soft and lines are broadened; *Suzaku* spectra confirm the lack of emission above 2 keV. Nor do the relative line shifts and widths suggest any wind decoupling by ions. The He-like triplets indicate that the bulk of the X-ray emission is formed rather close to the star, within five stellar radii. Our results challenge the idea that some OB stars are "weak-wind" stars that deviate from the standard wind–luminosity relationship. The wind is not weak, but it is hot and its bulk is only detectable in X-rays.

Key words: stars: early-type – stars: individual (mu Col) – stars: mass-loss – X-rays: stars

Online-only material: color figures

1. INTRODUCTION

The outflow of stellar winds from massive OB-type stars is an important process which affects both the chemical enrichment and kinetics of the interstellar medium (e.g., Leitherer et al. 1992). The mass loss itself is enough to change the evolution of the star, which ends its life in a supernova explosion, also profoundly changing its environment. Hence, quantitative understanding of massive star winds is important not only as a basic component of stellar astrophysics, but also for understanding cosmic feedback on galactic scales throughout cosmic history.

While some basic physics of stellar winds in massive stars is well established–that winds are accelerated by photoelectric absorption of the intense ultraviolet radiation field by a multitude of metal lines and that an instability can lead to wind shocks which generate X-rays–there are still puzzles to be solved. One of these is the "weak-wind" problem in which UV line diagnostics clearly show a wind signature in classical P Cygni line profiles, but modeled mass-loss rates can be discrepant by more than an order of magnitude from values expected based on O star statistical trends and theoretical foundations, specifically the wind momentum–luminosity relation (e.g., Puls et al. 1996). Factors of a few in mass loss are enough to be significant for stellar evolution and cosmic feedback (e.g., Puls et al. 2008).

It has long been known that photoionization by X-rays can alter the ionization balance in the wind regions where the UV lines are formed (Waldron 1984; MacFarlane et al. 1993). There is a theoretical degeneracy in that different values of mass-loss rate ($\dot{M}$) and X-ray luminosity (L_x) can produce very similar UV line profiles (Puls et al. 2008; Marcolino et al. 2009); direct knowledge of the X-ray spectrum is thus important for reliable determination of wind parameters. Another possibility is that cool and hot plasma emission originate from different volumes or densities; that is, clumping can affect the interpretation (Hamann et al. 2008). μ Col belongs to the weak-wind domain defined by Lucy (2010) in which a star's rate of mechanical energy loss in a radiatively driven wind is less than the radiative output from nuclear burning; Lucy showed that there is a huge disparity between the theoretically expected $\dot{M}$ and values derived from UV and optical spectra. Lucy (2012) developed a phenomenological model and suggested that in low-luminosity O-type stars, the volumetric roles of hot and cool gas are possibly reversed compared to O-type stars of high luminosity; thus in the weak-wind stars, a larger volume is occupied by the hot gas than by the cool gas.

μ Col (HD 38666) is an O9.5 V runaway (and single) star and is one of the weakest wind Galactic O-type stars (e.g., see Figures 39 and 41 in Martins et al. 2005). These factors are what motivated our spectroscopic study of the prototypical weak-wind system, μ Col, at high resolution with *Chandra* and at low resolution but greater sensitivity at higher energies with *Suzaku*. In this Letter, we concentrate on the primary empirical results from the X-ray spectral analysis of μ Col. A subsequent paper will investigate the influence of the X-rays on the cool wind component (H. Todt et. al., in preparation).

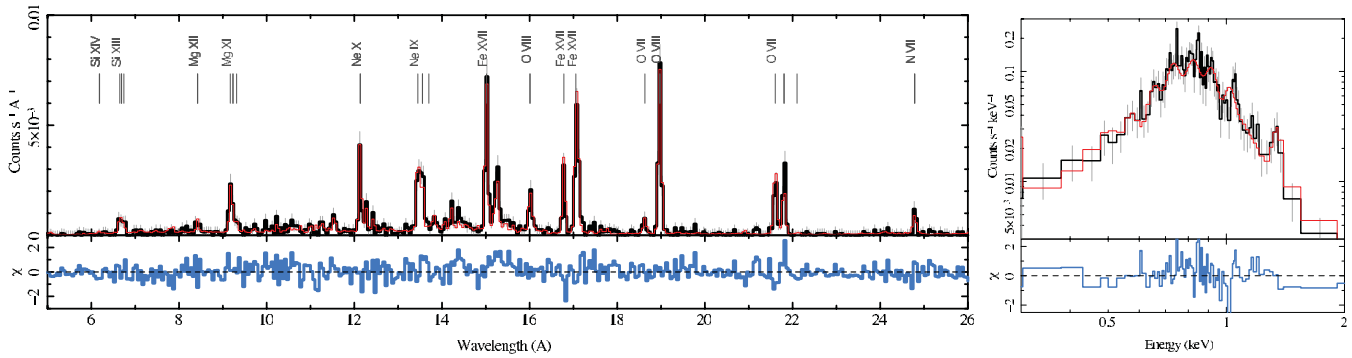

Figure 1. μ Col *Chandra*/LETG/ACIS spectrum (left); black: observed count rate; thin-gray line (red in the online version): model; the lower panel shows the χ^2 residuals against a broken power-law APEC model modified for photoexcitation of triplets. Lines are broader than the instrumental width. The *Suzaku* spectrum is shown on the right (black). For conciseness, we have summed the counts from the three detectors; such is not recommended when fitting, but it provides a good summary visualization of the data. The folded *Chandra*-derived model is in gray (red in the online version), and residuals below. We emphasize that the *Chandra*-derived model was not fit to the *Suzaku* spectrum, only folded through the response to provide model counts and residuals; the model agrees very well without any adjustments. It is significant that there is little or no flux detected above 2 keV where *Suzaku* has substantial sensitivity.

(A color version of this figure is available in the online journal.)

Table 1
μ Col Properties

Property	Value	Property	Value
Spectral type	O9.5 V	d (pc)[a]	408
$T_{\rm eff}$ (K)[b]	33000	$R/R_\odot$[b,c]	4.6
$\log(L_{\rm bol}/L_\odot)$[b,c]	4.4	v_∞ (km s^{-1})[b]	1200
$\dot{M}_{uv}$ ($M_\odot$ yr^{-1})[b]	$10^{-9.5}$	$N_{\rm H}$ (cm^{-2})[d]	5×10^{19}
f_x(1–40 Å) (cgs)[e,f]	6×10^{-13}	$\log(L_{\rm x}/L_{\rm bol})$[e]	−6.9
EM_x (cm^{-3})[e]	$10^{54.1}$	$T_{\rm max}$ (MK)[e]	4.4
$v_{\infty,x}$ (km s^{-1})[e]	1600 (±275)		
f/i(O VII)[g]	<0.01	r(O VII)[g]	<3.3
f/i(Ne IX)[g]	0.04–0.14	r(Ne IX)[g]	2.3–4.4
f/i(Mg XI)[g]	>0.2	r(Mg XI)[g]	>2.1

Notes.
[a] From the *Hipparcos* parallax, as re-evaluated by van Leeuwen (2007).
[b] Martins et al. (2005).
[c] Adjusted for the adopted distance.
[d] Cassinelli et al. (1994), Howk et al. (1999).
[e] This work.
[f] The flux is as observed at Earth, with foreground absorption.
[g] f/i gives the ratio of the forbidden to intercombination line fluxes, and r is the radius of formation in units of the stellar radius, as derived from PoWR models.

2. ANALYSIS

We have obtained a 232 ks exposure of μ Col with the *Chandra* LETG/ACIS instrument (Obs2IDs 12349, 12350, 13422, PI: L. Oskinova). Figure 1 shows the count-rate spectrum. Since μ Col is a single star, there are no ambiguities present as when interpreting observations of binary systems with composite spectra or colliding wind emission. Relevant stellar properties are given in Table 1.

There are several key X-ray spectral stellar wind diagnostics. The line profile is sensitive to the wind opacity and velocity field (MacFarlane et al. 1991; Owocki & Cohen 2001); the line centroid and width are useful proxies, being sensitive to wind parameters governing the detailed line shape. Emission-line strengths are indicative of plasma temperatures and elemental abundances. The continuum at the shortest wavelengths available (2–10 Å, 1–6 keV) is also very sensitive to the highest temperatures present. The He-like triplets are sensitive to electron density and the UV radiation field through collisional and photoelectric excitation which can depopulate the forbidden-line level, weakening it while strengthening the intercombination lines (Gabriel & Jordan 1969; Blumenthal et al. 1972); in O stars, the UV field typically dominates the depopulation and hence He-like line ratios are diagnostic of radius of formation (Waldron & Cassinelli 2001). Very close to the photosphere, density effects could also become significant.

We have fit a global model to the X-ray spectrum, using standard products produced by CIAO (version 4.3 and associated calibration database; Fruscione et al. 2006), using ISIS (Houck & Denicola 2000), and the collisional ionization equilibrium emissivities in AtomDB (version 2.0; Smith & Brickhouse 2008). For the plasma model, we used a broken power-law emission measure distribution (EMD; which in differential form is defined as $n_e n_h dV/dT$), with variable abundances for significant ions, a Doppler shift, and line profiles defined by a global Gaussian–Doppler broadening term. Our models show that the absorption of X-rays in the cool stellar wind is negligible and spectra can be well fit neglecting wind absorption. Abundances, velocity, and broadening were common over all temperature components. The resulting fit is shown as the red curve in Figure 1. The EMD is shown in Figure 2.

Abundances (referenced to solar photospheric values of Asplund et al. 2009) were about half of solar (O, Si, and Fe) or near solar (N, Ne)—we could not obtain a good fit using abundances all set to solar. This may be due to the adopted smooth functional form of the EMD, since the EMD and abundances are somewhat degenerate. Trial fits with discrete temperature components were also poorer when using solar abundances. To explore this somewhat further, since the integrated emission measure is fundamental to our main result, we evaluated the 90% confidence limits of the model normalization, froze this at each of the high and low limits, and re-fit the spectrum to obtain new EMD and abundances. We could have half the integrated EM with relative abundances increased to 0.7–1.5, or we could have about triple the best-fit EM, also with slightly modified abundances. (We note that from UV spectra, Fitzpatrick & Massa (1999) also found low abundances for μ Col, but did not believe their results plausible and attributed them to model deficiencies.)

The broken power-law model is empirically justified in that it provides a necessary multi-thermal model and does fit well with relatively few parameters. Such an EMD can be physically justified by hydrodynamic shock models which predict a wide

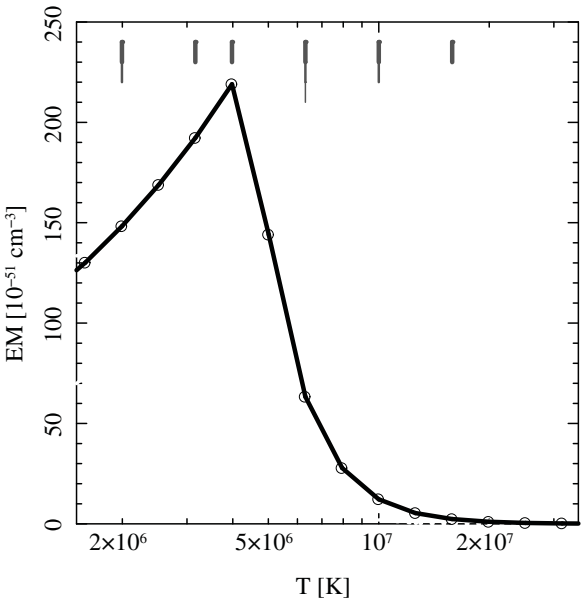

Figure 2. Best-fit emission measure distribution is given by the thick solid line. Circles mark the 1 dex temperature intervals, the resolution of the emmissivity database, and the value plotted is the emission measure integrated over 0.1 dex. Vertical bars near the top mark the temperatures of maximum emissivity for detected emission lines, and the abscissa's range spans the temperatures where these lines have greater than 50% of their maximum emissivity. The instruments have significant sensitivity from 3–6 Å such that EM above 10^7 K would be apparent in lines and continuum.

(A color version of this figure is available in the online journal.)

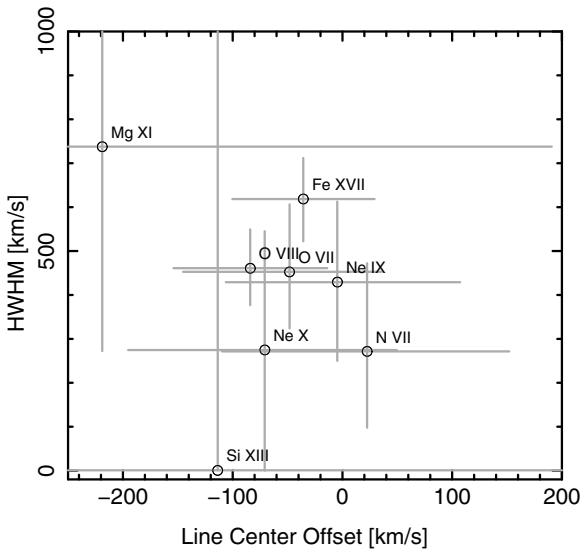

Figure 3. μ Col emission-line Doppler offset and width; error bars give 90% confidence limits. Due to lower resolution at shorter wavelengths, the Mg XI and Si XIII lines are poorly constrained. The systemic line-of-sight velocity of 109.2 km s^{-1} (Evans 1967) has been removed.

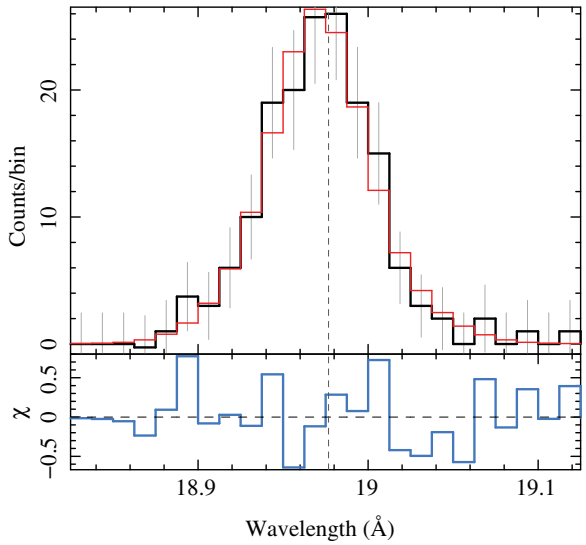

Figure 4. μ Col O VIII profile (black), wind-profile fit (gray; red in the online version), and residuals (lower panel). The model has a line center offset of 24 (±54) km s^{-1}, and v_∞ = 1600 (±275) km s^{-1}. The model profile was for $\beta = 0.7$, $R_0/R_\star = 1.1$, with a smooth, unclumped wind.

(A color version of this figure is available in the online journal.)

range of temperatures over a large range of radii (Feldmeier et al. 1997). Other OB-stars have also shown similar, empirically determined EMD (Wojdowski & Schulz 2005). The important point here is to obtain an order-of-magnitude estimate of the EM and that can be done with a variety of plausible models. Also given that the X-ray emitting plasma is optically thin, it does not matter (for the EMD) where the emission originates, under the assumption that abundances are independent of temperature and density.

Model properties are given in Table 1; the volume emission measure, EM$_x$, is integrated over the temperature range from 1–100 MK.

We have observed μ Col using the *Suzaku* satellite for 26 ks (ObsID 405059010, PI: L. Oskinova). We used the HEASoft 6.9 and the CALDB xis20100123 for the X-ray Imaging Spectrometer (XIS) analysis; the Hard X-ray Detector (HXD) did not detect any signal. The *Suzaku* spectrum is consistent with the above model, with no flux above 2 keV. Figure 1 shows the *Suzaku* spectrum, the folded *Chandra*-derived model, and residuals; there is good agreement.

Global fits cannot necessarily provide detailed information present in individual lines, particularly if lines from different ions have different characteristics from local conditions (e.g., velocity and temperature gradients). Hence, we also fit the stronger lines in the LETG/ACIS spectrum with Gaussians (folded through the instrument response), with a continuum derived from the global plasma model. The parameters relevant here are the centroids and widths (Figure 3). A non-zero centroid indicates a wind, being skewed to the blue by disk occultation of the receding wind and by absorption in the wind.

We also computed a model line shape for an expanding wind (Oskinova et al. 2006) and fit this to the strongest, isolated feature in the spectrum, O VIII (18.967, 18.973 Å) by adjusting the line position, flux, and scaling the width (Figure 4). We used an unclumped model profile with $\beta = 0.7$ and $R_0/R_\star = 1.1$. We find the wind is thin enough that a small asymmetry and a shift are due to the stellar disk occultation of the receding hot wind. The blueshift in the Gaussian fit to O VIII of −84 km s^{-1} (Figure 3) is consistent with the wind profile model, whose best fit is at the expected line position (i.e., no offset, within one standard deviation accuracy of 50 km s^{-1}). We did not achieve a good fit for the UV-derived v_∞ = 1200 km s^{-1}, but had to increase the hot wind velocity to 1600 (±275) km s^{-1}. UV spectra do not allow precise determination of v_∞; published values range from 1000 to 2000 km s^{-1} (Martins et al. 2005). Our PoWR models showed that the C IV, Si IV, and N V lines can be equally well fit with v_∞ of 1200 km s^{-1} or 1600 km s^{-1}. We

can also achieve an equally good fit to O VIII for $\beta = 1$, but with $v_\infty = 2800\,\mathrm{km\,s^{-1}}$. More detailed analysis with more lines and a variety of model assumptions are required. For a conservative approach, we prefer the lower v_∞.

The final line measurements of use are the He-like triplet ratios. We have measured these for O VII, Ne IX, and Mg XI (Si XIII is too weakly exposed and significantly blended to be useful). The forbidden lines are much weakened: The O VII forbidden line was not detected, and the Ne IX forbidden line was very weak. In both cases, the intercombination lines are as strong as the resonance lines. The forbidden-to-intercombination ratios (f/i) provide limits on the radii of formation. We applied a simple model assuming triplet formation occurs at a single radius in the wind, using only excitation by photospheric UV fluxes from model atmospheres such as TLUSTY or ATLAS-9 (Lanz & Hubeny 2003, 2007; Kurucz 1979). We also used more sophisticated treatment using the PoWR code (Hamann & Gräfener 2004) in which the wind model calculates ionization structure, solves the energy equation, includes X-rays, includes photospheric emission corrected for absorption lines, line blanketing, non-LTE populations, stellar disk limb darkening, and the diffuse UV radiation field. Each of the methods predicts the f/i ratio versus radius r of formation. Values (which were nearly identical for all methods) are given in Table 1 with r, in units of the stellar radius.

There is some temperature dependence in the triplet ratios, but it is below 10%, less than our measurement uncertainty. The point-formation model also ignores the effect of any distributed emission. If there is contribution from further out in the wind, our f/i-derived radii will be overestimates (since f increases and i decreases at larger radii—the distributed emission ratio would be larger than at any point at smaller radius).

We have also looked for variability. The count rate in dispersed photons appears constant; the rate cannot change by more than 5%–10% in time intervals of 1 ks or more.

3. "WEAK-WIND" STARS ARE NOT LOW MASS-LOSS WINDS

The He-like triplets place the X-ray emission within about 2–5 stellar radii of the photosphere. Line widths are consistent with X-rays being formed at small radii. We assume that the hot plasma obeys the continuity equation, that the standard velocity law holds for the hot plasma, namely $v_x = v_{\infty,x}(1 - bR_*/r)^\beta$, and that the hot plasma exists only above some inner radius $R_0 \geqslant R_*$. For $v_\infty = 1200\,\mathrm{km\,s^{-1}}$, $b = 0.97$ (a value based on the ratio of the sound speed at $R_\star$ to v_∞, which provides a non-zero wind velocity, but which is somewhat uncertain), and $\beta = 1$, we expect wind velocities in this region to be about 800–1300 km s^{-1}. Figure 3 shows the widths to be somewhat smaller at 300–700 km s^{-1}. This suggests that much of the X-ray emission originates very close to the star within the radiation-driven wind acceleration zone, or that the hot plasma does not follow the typical velocity law. The hot plasma, however, does expand with relatively high velocity since the X-ray emission line profiles are resolved. Detailed line-profile fitting using wind models will be required to determine the structure in more detail.

With the assumptions above and the definition of the X-ray emission measure (and $\beta = 1$ to allow an analytic integration), we can derive a simple expression for the X-ray-inferred mass-loss rate in solar masses per year, also assuming that the hot wind is unclumped and that the cool wind is optically thin to X-rays (as justified by the line profiles):

$$\dot{M}_x = 3 \times 10^{-9}\, v_{\infty,x} \left[\frac{R_\star}{R_\odot}\, \mathrm{EM}_x \left(\frac{R_0}{R_\star} - b \right) \right]^{1/2} \qquad (1)$$

in which $v_{\infty,x}$ is the hot wind's terminal velocity as determined from X-ray emission line profiles (in units of 1000 km s^{-1}), $R_\star$ is the stellar radius, EM_x is the emission measure of the hot plasma (in units of 10^{54} cm^{-3}), and b is the unitless parameter from the wind velocity law. Using $R_0 = R_\star$, $b = 0.97$, and values from Table 1, we infer that $\dot{M} \approx 2 \times 10^{-9}\, M_\odot\,\mathrm{yr}^{-1}$. This is six times the value derived from the UV by Martins et al. (2005; or more, accounting for subsequent revisions in distance and stellar radius). If the hot wind begins somewhere above the photosphere, then the inferred mass–loss rate will be even larger (e.g., about 20 times for $R_0/R_\star = 1.5$).

The above $\dot{M}_x$ uses our $\mathrm{EM}_x \sim 10^{54}$. If were to assume the much lower $\dot{M}_{uv}$, we would infer a much smaller emission measure for a spherically symmetric wind. This means that most of the wind is hot (or denser) than the UV-emitting plasma, a situation also noticed in the study of main-sequence B stars (e.g., Cassinelli et al. 1994).

We conclude that the hot wind of μ Col must have a larger volume or greater density than the cool wind. The wind is not weak, but it is hot and its bulk is only detectable in X-rays.

Our observations exclude other proposed weak-wind explanations, such as magnetically channeled wind shocks (MCWS) or frictionally decoupled winds. The X-ray spectrum of μ Col is not characteristic of MCWS in which hot plasma is held in stationary structures close to the stellar photosphere and which reach high temperatures from collision of funneled high-velocity winds (Babel & Montmerle 1997; Townsend et al. 2007). The plasma of μ Col is not extremely hot ($T \gtrsim 10$ MK) nor are lines unshifted and unresolved. Decoupling of ions from neutrals could occur at low densities or very low metallicities, creating a two-fluid system (cf. Springmann & Pauldrach 1992; Krtička & Kubát 2001; Martins et al. 2004). Frictional heating by decoupled ions seems unlikely: the plasma is not extremely cool ($\lesssim$1 MK) with different widths and velocities for different ions (within our sensitivity; Figure 3). Given the X-ray EM_x and likely radii of formation, the density is not as low as once presumed. The relative Fe abundance from our fits is about 0.5 solar, not low enough to cause decoupling.

Lucy (2010) reduced the weak-wind discrepancy through theoretical arguments. The X-ray spectra of μ Col support this with empirical evidence for a dominant hot wind, even given some uncertainty from still poorly determined factors of clumping, wind velocity law, and location of the wind base. Drew et al. (1994) suggested that X-rays may increase the wind ionization at the critical point, lowering the effective radiative acceleration and mass-loss rate. Our *Chandra* observations resolve the broad X-ray emission lines, indicating that the hot plasma expands at high velocities, perhaps even exceeding the cool wind velocity determined from UV spectra.

Our empirical findings, reached in ignorance of work by Lucy (2012), are in line with his claim that in late-type O-dwarfs the ambient wind is heated to temperatures of few MK at radii $>1.4\,R_*$, with cool radiatively driven gas being confined to dense clumps and small volume filling factor. Further out in the wind in his model, cool clumps are destroyed by heat conduction from the hot plasma, and the outflow is dominated by a hot thermal wind which reaches a supersonic terminal velocity of $\sim$1000 km s^{-1}.

In future work, we will refine our order-of-magnitude estimates using detailed wind models. For a relatively thin wind, we do not expect significant qualitative changes. Some observational uncertainties need to be refined: we only have both upper and lower limits for the formation radii of Ne IX; whether other species form at 5 R_* or below 2 R_* is important for wind shock models. Higher spectral resolution would be of use, especially for the hottest He-like triplet in the spectrum, Si XIII, to probe the deepest layers. Higher resolution would better determine line shifts and widths, and better constrain wind structure.

Najarro et al. (2011) recently classified σ Ori AB (HD 37468, O9.5 V + B0.5 V) as a weak-wind system, based on infrared spectra, revising its mass-loss rate downward by more than two orders of magnitude from that in Howarth & Prinja (1989). This star has also been observed at high resolution in X-rays (Waldron & Cassinelli 2007; Zhekov & Palla 2007; Skinner et al. 2008). Based on these prior works and our own analysis of the *Chandra*/HETG spectrum, we find that σ Ori has X-ray spectral characteristics very similar to those of μ Col. This further corroborates our conclusions that the weak-wind phenomenon is due to a property of the cool plasma being a minor constituent of the wind.

4. CONCLUSIONS

Our results challenge the idea that some OB stars are "weak-wind" stars that deviate from the standard wind–luminosity relationship. From high-resolution X-ray spectrum of μ Col, specifically He-like lines and the total emission measure, this star does not appear unusual relative to other O stars except for its weak-wind status. Its X-ray emission measure, line widths, and centroids are in good agreement with the OB main-sequence star results of Waldron & Cassinelli (2007). The volume emission measure of the X-ray emitting plasma must be very much larger than the cool, UV-emitting plasma, and we believe that the weak-wind problem is reduced or eliminated when the hot and dominant component of the wind is taken into account. The wind is not weak, but it is hot and its bulk is only detectable in X-rays.

Support for this work was provided by the National Aeronautics and Space Administration through Chandra Award Numbers GO1-12017A (WLW), GO1-12017B (DPH), and GO1-12017C (RI) issued by the Chandra X-ray Observatory Center, which is operated by the Smithsonian Astrophysical Observatory for and on behalf of the National Aeronautics Space Administration under contract NAS8-03060. L.M.O. was funded by DLR grant FKZ 50 OR 1101. We thank W.-R. Hamann for comments and help with PoWR code.

Facilities: CXO (LETG/ACIS), Suzaku

REFERENCES

Asplund, M., Grevesse, N., Sauval, A. J., & Scott, P. 2009, ARA&A, 47, 481
Babel, J., & Montmerle, T. 1997, ApJ, 485, L29
Blumenthal, G. R., Drake, G. W. F., & Tucker, W. H. 1972, ApJ, 172, 205
Cassinelli, J. P., Cohen, D. H., MacFarlane, J. J., Sanders, W. T., & Welsh, B. Y. 1994, ApJ, 421, 705
Drew, J. E., Hoare, M. G., & Denby, M. 1994, MNRAS, 266, 917
Evans, D. S. 1967, in IAU Symp. 30, Determination of Radial Velocities and their Applications, ed. A. H. Batten & J. F. Heard (London: Academic), 57
Feldmeier, A., Puls, J., & Pauldrach, A. W. A. 1997, A&A, 322, 878
Fitzpatrick, E. L., & Massa, D. 1999, ApJ, 525, 1011
Fruscione, A., McDowell, J. C., Allen, G. E., et al. 2006, Proc. SPIE, 6270, 62701V
Gabriel, A. H., & Jordan, C. 1969, MNRAS, 145, 241
Hamann, W.-R., Feldmeier, A., & Oskinova, L. M.(ed.) 2008, Clumping in Hot-Star Winds (Potsdam: Univ. Potsdam)
Hamann, W.-R., & Gräfener, G. 2004, A&A, 427, 697
Houck, J. C., & Denicola, L. A. 2000, in ASP Conf. Proc. 216, Astronomical Data Analysis Software and Systems IX, ed. N. Manset, C. Veillet, & D. Crabtree (San Francisco, CA: ASP), 591
Howarth, I. D., & Prinja, R. K. 1989, ApJS, 69, 527
Howk, J. C., Savage, B. D., & Fabian, D. 1999, ApJ, 525, 253
Krtička, J., & Kubát, J. 2001, A&A, 377, 175
Kurucz, R. L. 1979, ApJS, 40, 1
Lanz, T., & Hubeny, I. 2003, ApJS, 146, 417
Lanz, T., & Hubeny, I. 2007, ApJS, 169, 83
Leitherer, C., Robert, C., & Drissen, L. 1992, ApJ, 401, 596
Lucy, L. B. 2010, A&A, 512, A33
Lucy, L. B. 2012, A&A, 544, A120
MacFarlane, J. J., Cassinelli, J. P., Welsh, B. Y., et al. 1991, ApJ, 380, 564
MacFarlane, J. J., Waldron, W. L., Corcoran, M. F., et al. 1993, ApJ, 419, 813
Marcolino, W. L. F., Bouret, J.-C., Martins, F., et al. 2009, A&A, 498, 837
Martins, F., Schaerer, D., Hillier, D. J., & Heydari-Malayeri, M. 2004, A&A, 420, 1087
Martins, F., Schaerer, D., Hillier, D. J., et al. 2005, A&A, 441, 735
Najarro, F., Hanson, M. M., & Puls, J. 2011, A&A, 535, A32
Oskinova, L. M., Feldmeier, A., & Hamann, W. 2006, MNRAS, 372, 313
Owocki, S. P., & Cohen, D. H. 2001, ApJ, 559, 1108
Puls, J., Kudritzki, R.-P., Herrero, A., et al. 1996, A&A, 305, 171
Puls, J., Vink, J. S., & Najarro, F. 2008, A&AR, 16, 209
Skinner, S. L., Sokal, K. R., Cohen, D. H., et al. 2008, ApJ, 683, 796
Smith, R., & Brickhouse, N. S. 2008, BAAS, 40, 186
Springmann, U. W. E., & Pauldrach, A. W. A. 1992, A&A, 262, 515
Townsend, R. H. D., Owocki, S. P., & Ud-Doula, A. 2007, MNRAS, 382, 139
van Leeuwen, F. 2007, A&A, 474, 653
Waldron, W. L. 1984, ApJ, 282, 256
Waldron, W. L., & Cassinelli, J. P. 2001, ApJ, 548, L45
Waldron, W. L., & Cassinelli, J. P. 2007, ApJ, 668, 456
Wojdowski, P. S., & Schulz, N. S. 2005, ApJ, 627, 953
Zhekov, S. A., & Palla, F. 2007, MNRAS, 382, 1124